Video Article

In Vivo, Percutaneous, Needle Based, Optical Coherence Tomography of Renal Masses

Peter G. Wagstaff[1], Abel Swaan[2], Alexandre Ingels[1], Patricia J. Zondervan[1], Otto M. van Delden[3], Dirk J. Faber[2], Ton G. van Leeuwen[2], Jean J. de la Rosette[1], Daniel M. de Bruin[1,2], M. Pilar Laguna Pes[1]

[1]Department of Urology, Academic Medical Center

[2]Department of Biomedical Engineering and Physics, Academic Medical Center

[3]Department of Radiology, Academic Medical Center

Correspondence to: Peter G. Wagstaff at p.g.wagstaff@amc.nl

URL: http://www.jove.com/video/52574
DOI: doi:10.3791/52574

Keywords: Medicine, Issue 97, Optical Coherence Tomography, OCT, Optical frequency domain imaging, OFDI, Optical biopsy, Needle based, Percutaneous, Renal mass, Kidney tumor, Kidney cancer.

Date Published: 3/30/2015

Citation: Wagstaff, P.G., Swaan, A., Ingels, A., Zondervan, P.J., van Delden, O.M., Faber, D.J., van Leeuwen, T.G., de la Rosette, J.J., de Bruin, D.M., Laguna Pes, M.P. *In Vivo*, Percutaneous, Needle Based, Optical Coherence Tomography of Renal Masses. *J. Vis. Exp.* (97), e52574, doi:10.3791/52574 (2015).

Abstract

Optical coherence tomography (OCT) is the optical equivalent of ultrasound imaging, based on the backscattering of near infrared light. OCT provides real time images with a 15 µm axial resolution at an effective tissue penetration of 2-3 mm. Within the OCT images the loss of signal intensity per millimeter of tissue penetration, the attenuation coefficient, is calculated. The attenuation coefficient is a tissue specific property, providing a quantitative parameter for tissue differentiation.

Until now, renal mass treatment decisions have been made primarily on the basis of MRI and CT imaging characteristics, age and comorbidity. However these parameters and diagnostic methods lack the finesse to truly detect the malignant potential of a renal mass. A successful core biopsy or fine needle aspiration provides objective tumor differentiation with both sensitivity and specificity in the range of 95-100%. However, a non-diagnostic rate of 10-20% overall, and even up to 30% in SRMs, is to be expected, delaying the diagnostic process due to the frequent necessity for additional biopsy procedures.

We aim to develop OCT into an optical biopsy, providing real-time imaging combined with on-the-spot tumor differentiation. This publication provides a detailed step-by-step approach for percutaneous, needle based, OCT of renal masses.

Video Link

The video component of this article can be found at http://www.jove.com/video/52574/

Introduction

The past decades have shown a steady increase in the incidence of renal masses [1,2]. Until now, renal mass treatment decisions have been made primarily on the basis of MRI and CT imaging characteristics, age and comorbidity. However these diagnostic methods and clinical parameters lack the finesse to truly detect the malignant potential of a renal mass. A core biopsy or fine needle aspiration with sufficient tissue for pathological evaluation (diagnostic) provides objective tumor differentiation with both sensitivity and specificity in the range of 95-100% [3]. Therefore biopsy is gaining acceptance in the evaluation of suspicious renal masses [4,5]. However, biopsies without sufficient tissue to establish a diagnosis or with normal renal parenchyma (non-diagnostic) occur at a rate of 10-20% overall, and even up to 30% in small renal masses (<4 cm, SRMs), delaying the diagnostic process due to the frequent necessity for additional biopsy procedures[3,5].

Optical coherence tomography (OCT) is a novel imaging modality that has the potential to overcome the aforementioned hurdles in renal mass differentiation. Based on the backscattering of near infrared light, OCT provides images with a 15 µm axial resolution at an effective tissue penetration of 2-3 mm (**Figure 1**, **2**). The loss of signal intensity per millimeter of tissue penetration, a resultant of tissue-specific light scattering, is expressed as the attenuation coefficient (μ_{OCT}: mm^{-1}) as described by Faber *et al.* [6]. Histological characteristics can be correlated to μ_{OCT} values providing a quantitative parameter for tissue differentiation (**Figure 3**).

During carcinogenesis, malignant cells display an increased number, larger and more irregularly shaped nuclei with a higher refractive index and more active mitochondria. Due to this overexpression of cell components, a change in μ_{oct} is to be expected when comparing malignant tumors to benign tumors or unaffected tissue [7].

Recently we studied the ability of superficial OCT to differentiate between benign and malignant renal masses [8,9]. In 16 patients, intra-operative OCT measurements of tumor tissue were obtained using an externally placed OCT probe. The control arm comprised of OCT measurements of unaffected tissue in the same patients. Normal tissue showed a significantly lower median attenuation coefficient compared to malignant tissue,

confirming the potential of OCT for tumor differentiation. This quantitative analysis has been applied in a similar fashion to grade other types of malignant tissue, such as urothelial carcinoma [10,11] and vulvar epithelial neoplasia differentiation [12].

We aim to develop OCT into an optical biopsy, providing real-time imaging combined with on-the-spot tumor differentiation. The goal of the current study is to describe a percutaneous, needle based, OCT approach in patients diagnosed with a solid enhancing renal mass. This method description is, to our knowledge, the first to assess the possibility of needle based OCT of renal tumors.

Protocol

The presented procedure takes place under a research protocol approved by the Institutional Review Board of the Academic Medical Center Amsterdam, registration number NL41985.018. Written informed consent is required from all participants.

1. System

1. For this experiment, use a Fourier domain OCT system, operating at a 1,280–1,350 nm wavelength band [13]. Fourier domain low-coherence interferometry allows for continuous scanning which increases the data acquisition speed when compared to the first generation time-domain OCT systems. Note: The OCT system is interfaced with a fiber optic probe, scanning helically at ~90° angle. It has an outer diameter of 2.7F (0.9 mm) and an insertable length of 135 cm. The probe connects to the OCT console through a drive motor and optical controller (mounting dock) with a pullback range of 54 mm. The acquired OCT datasets consist of 541 cross-sectional images (B-scans) with an axial resolution of 15 µm (**Figure 1**, **2**).
2. To guarantee accurate and reproducible attenuation measurements, calibrate by measuring μ_{oct} for increasing concentrations based on weight percentage of a fat emulsion, (*e.g.*, Intralipid) as described previously by Kodach *et al.*[14, 15].
   In short:
   1. Dilute a standard batch of 20% fat emulsion with demineralized H_2O to achieve concentrations of 0.125, 0.250, 0.5, 1.0, 2.0, 4.0, 10, 15 and 20 (stock) percent.
      1. Place the OCT probe in 200 ml of fat emulsion mixture and acquire an OCT measurement.
      2. Cross reference extracted μ_{oct} values with known values in literature.

2. Time Out and Patient Positioning

1. Prior to starting the procedure, perform a “time out” checking name, date of birth, procedure, procedural side, anticoagulant use, and allergies.
2. Depending on the tumor location, place the patient in either prone or lateral decubitus position. Provide the patient with adequate support and verify if he/she expects to be comfortable in this position over a 20 to 40 min period.
3. Using ultrasound (US)[16], localize the tumor and mark the needle entry point on the skin with permanent ink.
   NOTE: When using computed tomography (CT), use a flexible needle guidance template to localize the preferred position of the access needle.

3. Disinfection and Sterile Draping

1. Put on a surgical cap and mouth cover.
2. Clean the skin around the puncture site using a chlorhexidine/alcohol solution, taking care not to remove the previously placed needle entry mark (step 2.3). Disinfecting a wide area will prevent the necessity for additional cleaning in case of unexpected access needle repositioning.
3. With regard of the sterile content, open the percutaneous puncture set containing: a 10 ml syringe, a blunt aspiration needle, a 21 G injection needle, a scalpel, a 15 G co-axial introducer needle, a 18 G trocar needle, and a 16 G core biopsy gun.
4. Wash hands thoroughly, applying hand disinfectant afterwards. Put on a surgical gown and sterile gloves.
5. Cover the patient in sterile drapes.
6. Apply a sterile cover around the ultrasound probe and fix the needle guide in place.

4. OCT Preparation

1. Start the OCT console and enter the patient details in the fields labeled patient ID, last name, first name and DOB (date of birth) using the console interface.
2. With regard of the sterile content, unpack the OCT package containing an OCT probe, a sterile mounting dock cover, and a 5 ml luer-lock syringe.
3. Apply the sterile cover to the OCT console mounting dock. Guiding the non-sterile mounting dock requires the help of an assistant.
4. Fill the 5 ml syringe with 0.9% NaCl and attach it to the flushing port. Flush the OCT probe until water appears in the distal part of the probe cover.
5. Load the OCT probe into the mounting dock. After loading the probe will rotate and emit red light confirming proper functioning. Leave the probe in its protective cover during flushing and loading to minimize the risk of damage.
6. Remove the OCT probe from its cover. Place the probe on a hard surface and use a scalpel to shorten the tip. Fix the distal part of the probe during cutting in order to minimize pressure on the optical fiber and prism. Cut 5 mm distal from prism, using the emitted (red) light for orientation.

5. Puncture

1. Anesthetize the skin and deep layers using 2% lidocaine (20 mg/ml). Wait several minutes allowing for the lidocaine to take effect. Ask the patient if there is any pain.
2. Using the needle guide, place the 15 G co-axial introducer needle verifying the position through imaging. If placement is satisfactory, remove the obturator (sharp needle core).
3. Place the 18 G trocar needle through the introducer needle, piercing the tumor. Again verify the position of the needle with imaging. If placement is satisfactory remove the obturator.
4. Feed the OCT probe up the trocar needle until feeling resistance.
5. While fixing the OCT probe, retract the trocar needle, exposing the OCT probe to the tumor tissue. Keeping the tip of the trocar needle within the tumor minimizes kinking of the OCT probe during breathing cycles. This lowers the risk of probe damage.
6. OCT Scan:
    1. Perform an OCT scan, with the console set at 541 B-scans per dataset. The OCT system used here will perform an automated pullback over a length of 5.4 cm requiring no specific parameter adjustments.
    2. Check the scan for quality, artefacts and the appearance of solid tissue (**Figure 1A**). Artefacts most commonly appear as circular bands standing out from the normal OCT pattern (**Figure 1B**).
    3. Replace the probe if artefacts persists after rescanning.
7. Repeat step 5.6 until a minimum of 3 OCT datasets are acquired.
8. Remove the OCT probe and trocar needle, leaving the introducer needle in-place.
9. Arm the core biopsy gun and place it through the introducer needle, verifying the position on imaging.
10. If the positioning is satisfactory, fire the biopsy gun.
11. Place biopsy material in container according to pathology department protocol. Here, place biopsies on a petri dish with a paper inlay, sufficiently saturated with 0.9% NaCl.
12. Check the core biopsy quality and repeat step 5.9 and 5.10 until sufficient material is obtained.

Representative Results

Among the first 25 tumors (23 patients), a total of 24 successful OCT procedures were performed. In one case a probe malfunction led to the inability to acquire an OCT scan. Two adverse events (AE) occurred, which are described in detail in the discussion section. General patient characteristics are found in **Table 1**.

The OCT console has pre-installed software providing real-time OCT images for immediate qualitative analysis of acquired datasets. For further analysis and attenuation measurements, the OCT data can be exported as raw data, TIFF, DICOM or AVI format. Quantitative analysis of μ_{oct} of the OCT data is done using in-house developed software.

Using planimetric software, a 3D volume is rendered from the RAW data (**Figure 2A**). This provides a 3D overview of the scanned trajectory with the possibility of orthoslicing along 3 axes. The displayed dataset in **Figure 2** shows good quality over the full pullback length. A clear visual distinction can be made between solid tissue (**Figure 2B**-**C**), perirenal fat tissue (**Figure 2D**) and the inside of the trocar needle. Exported TIFF files are loaded into an ImageJ based software package to be viewed in 2D by scrolling through the stacked B-scans. Combining the 2D and 3D visualization of the OCT dataset a region of interest (ROI) is selected.

Within the ROI equally spaced B-scans are selected (**Figure 2**, **3**). Within the respective B-scans the attenuation coefficient is determined along a straight line radiating outward from the heart of the probe (**Figure 3A**, **D**). The ImageJ based software package has the option of plotting the data points along the attenuation line in a graph. The slope of the displayed graph represents the attenuation coefficient (**Figure 3B**, **E**).

By correlating attenuation measurements to histopathology results (**Figure 3C**, **F**), tissue specific cut-off values can be derived providing the means for tumor differentiation.

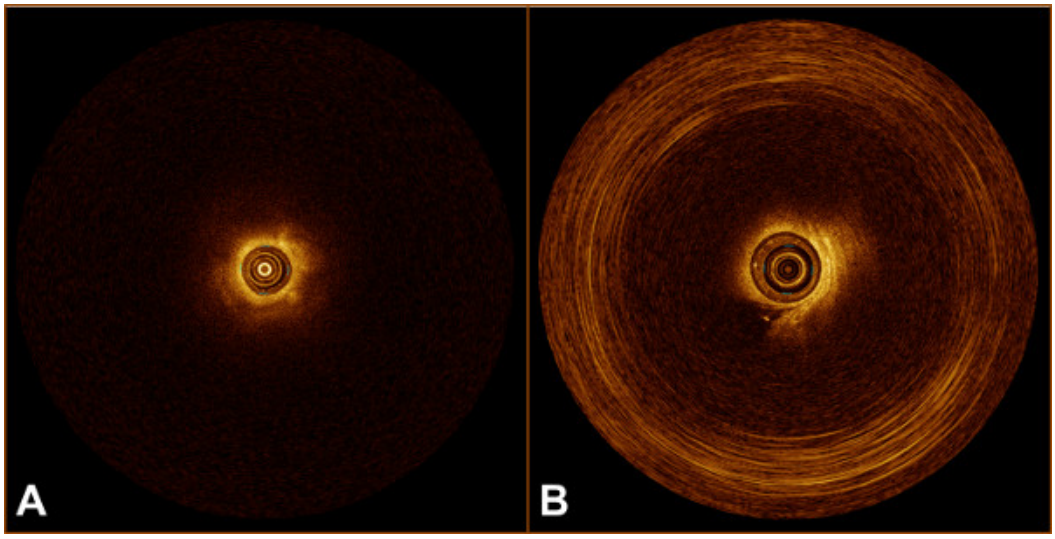

Figure 1: (**A**) OCT B-scan of solid tissue. B) OCT B-scan with circular artefact.

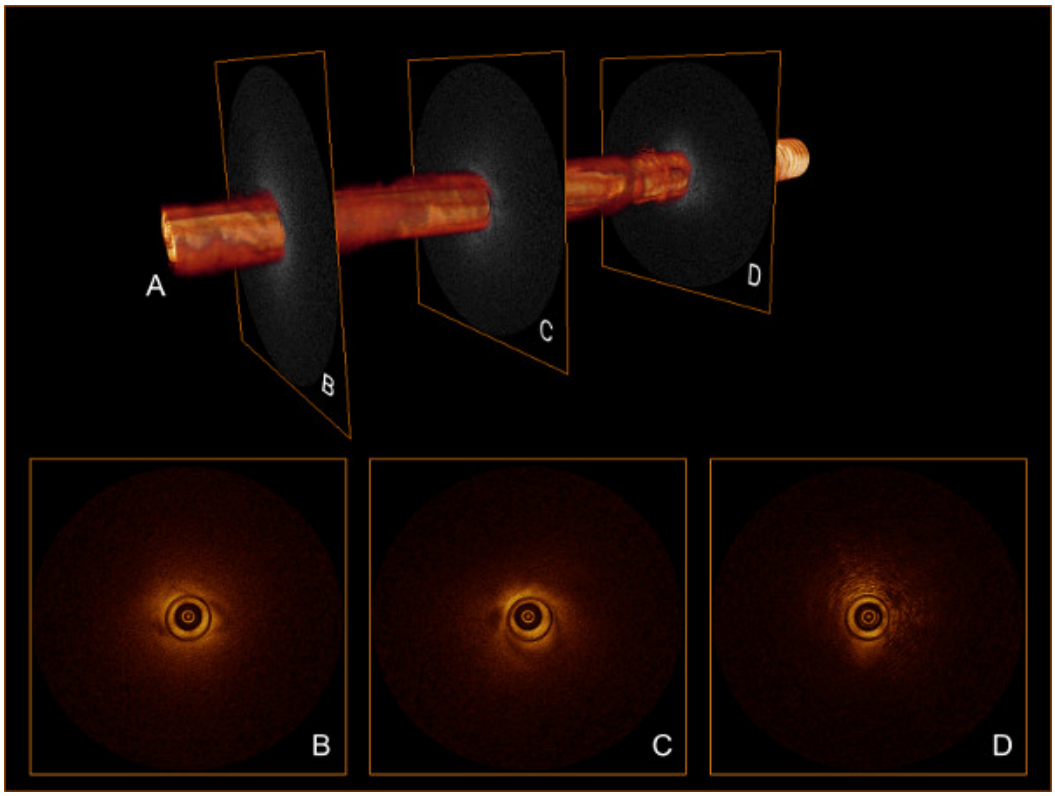

Figure 2: (**A**) 3D volume rendered from 541 stacked B-scans. (**B**-**C**) Selected B-scans showing solid tissue, indicating successful OCT probe placement. (**D**) Selected B-scan showing perirenal fat tissue.

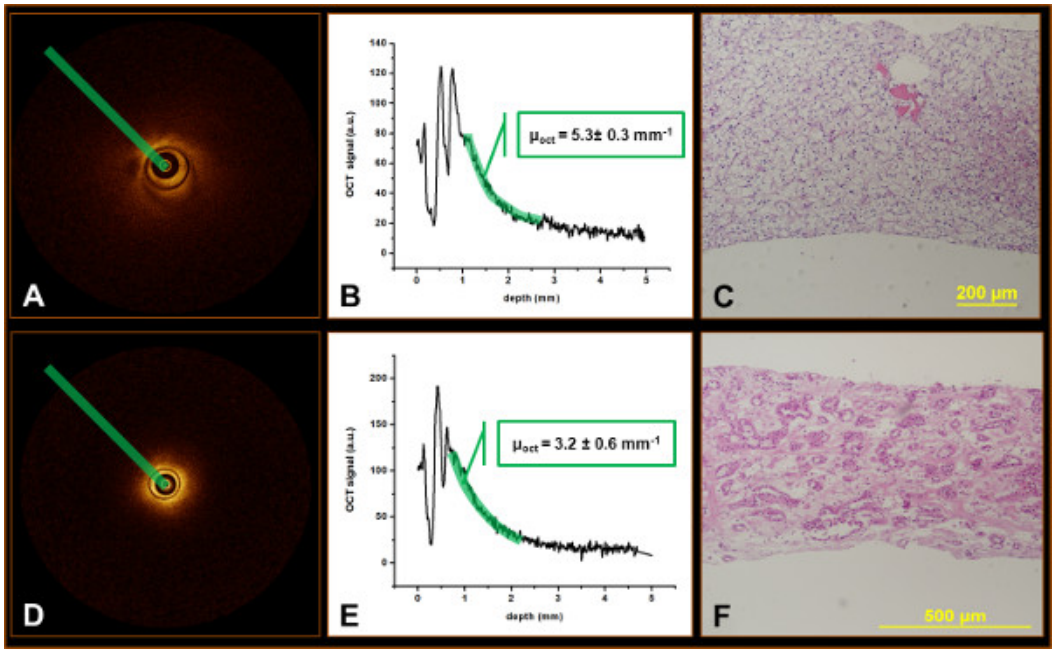

Figure 3: OCT analysis and correlation of a clear cell renal cell carcinoma (**A**-**C**) and an oncocytoma (**D**-**E**). Plotting the points along the highlighted line (**A**, **D**) provides the depicted graphs (**B**, **E**). The slope of the graphs represents the attenuation coefficient. Subsequently, the attenuation coefficient is correlated to the pathology specimen from the same location (**C**, **F**) in order to derive tissue specific cut-off values.

Patient No.	23
Tumor No.	25
Age (yrs): AVG (range)	63.7 (32-83)
Max tumor diameter (cm): AVG (range)	3.5 (1.4-7.5)
Sex	
Male (%)	17 (68)
Female (%)	8 (32)
Tumor side	
Left (%)	15 (60)
Right (%)	10 (40)
Tumor location	
Entirely above upper polar line or below lower polar line (%)	8 (32)
Crosses polar line (%)	9 (36)
>50% across polar line or crosses axial midline or between polar lines (%)	8 (32)
Exophytic / endophytic properties	
≥50% exophytic (%)	10 (40)
<50% exophytic (%)	14 (56)
Entirely endophytic (%)	1 (4)

Table 1: Patient characteristics.

Discussion

In this publication we report on the feasibility of percutaneous, needle based, OCT of the kidney. This is an essential first step in the development of OCT into a clinically applicable technique for tumor differentiation, termed as an “Optical Biopsy”. Our first 25 patients have shown percutaneous OCT to be an easy and safe procedure. An optical biopsy has two advantages over conventional core biopsies. First, the real time acquisition and analysis of OCT data will provide instant diagnostic results, compared to the 5-10 days of processing time of conventional pathology. Second, OCT has the potential to reduce the amount of non-diagnostic procedures, which is 20% for conventional biopsies. When an

OCT scan reveals perirenal fat or unaffected renal tissue (non-diagnostic results) the OCT operator can reposition the OCT probe to successfully target the tumor.

Two adverse events (AE) occurred among the first 25 patients. The first AE was post procedural hypotension, in a patient with known episodes of hypotension, which resolved after rest and 0.9% NaCl infusion.

In the second AE a fragment of the OCT probe tip sheared of. Requesting the patient to hold his breath during measurements prompted deep inspiration. Excessive kidney movement caused the OCT probe to kink and subsequently shear of on the edge of the trocar needle. A probe fragment of 1-2 mm remained in situ, yet caused no problems or discomfort. This AE took place during the OCT procedure of patient number 10. In the following patients the tip of the trocar needle was kept within the tumor (protocol step 5.5) minimizing kinking of the OCT probe, on the edge of the trocar needle, during breathing cycles. This modification of the OCT procedure has shown substantially less stress on the OCT probe. However, further prospective evaluation is necessary.

The OCT probe used in this study is designed for intravascular imaging of the coronary arteries. The possibility of automated pullback scanning combined with the 2.7 F (0.9 mm) diameter makes this probe suitable for needle based OCT of renal tumors. However, the delicate nature of the optical fiber and the prism fused to the distal tip make the probe susceptible to damage. In 3 cases, probe manipulation during the procedure caused probe failure, in 1 case before an OCT dataset could be acquired. Microscopic inspection of the prism showed no abnormalities, making a break in the optical fiber the most probable cause of failure.

Quantitative data analysis requires derivation of tissue specific attenuation cut-off values. This provides the means for objective tissue differentiation. We hypothesize that OCT is able to differentiate between benign and malignant lesions and subsequently between the 3 main malignant subgroups of renal cell carcinoma. Currently, attenuation values are calculated manually from selected areas of interest, which is a time consuming process. We have developed software for automated attenuation calculation. This reduces the inter- and intra-observer variability on ROI selection, speeds up the analysis process and increases the number of measurements per dataset. The integration of this software for instant attenuation coefficient calculation into the OCT console is a necessary future step in the development of a fully functional and clinically applicable optical biopsy technique.

In addition, a qualitative analysis protocol is necessary. Intra-procedural recognition of features of unaffected tissue (*i.e.* recognition of perirenal fat) could prompt OCT probe repositioning, reducing the number of non-diagnostic procedures. Furthermore, qualitative analysis is needed to select a ROI for attenuation coefficient calculation. Currently, we are developing a protocol consisting of predefined visual aspects to be scored. When sufficient datasets are acquired, blinded observers will validate this protocol.

The success of renal mass treatment strategies relies on accurate demarcation and profile determination, using smart treatment planning protocols and real time identification (subtyping and grading) and follow-up of the lesion. Both follow-up strategies and real-time identification of a lesion are unmet challenges using the current diagnostic techniques. OCT in the form of an optical biopsy has the potential to fulfil these requirements, providing minimal invasive analysis of carcinogenesis related change of optical properties and changes of layered tissue architecture *i.e.* visual detection of the structures in the OCT image.

Disclosures

The authors of this article have nothing to disclose.

Acknowledgements

This work is funded by the Cure for Cancer Foundation, Dutch Technology Foundation (STW) and The Netherlands Organisation for Health Research and Development (ZonMw).

References

1. Jemal, A., Siegel, R., Xu, J., Ward, E. Cancer statistics, 2010. *CA Cancer J. Clin.* **60**, 277-300 (2010).
2. Mathew, A., Devesa, S. S., Fraumeni, J. F., Chow, W. H. Global increases in kidney cancer incidence, 1973-1992. *Eur. J. Cancer Prev.* **11**, 171-178 (2002).
3. Volpe, A., *et al.* Contemporary management of small renal masses. *Eur. Urol.* **60**, 501-515 (2011).
4. Ljungberg, B., *et al.* EAU guidelines on renal cell carcinoma: the 2010 update. *Eur. Urol.* **58**, 398-406 (2010).
5. Donat, S. M., *et al.* Follow-up for Clinically Localized Renal Neoplasms. *AUA Guideline, J. Urol.* **190**, 407-416 (2013).
6. Faber, D. J., van der Meer, F. J., Aalders, M. C. G., van Leeuwen, T. G. Quantitative measurement of attenuation coefficients of weakly scattering media using optical coherence tomography. *Optics Express.* **12**, 4353-4365 (2004).
7. Xie, T. Q., Zeidel, M. L., Pan, Y. T. Detection of tumorigenesis in urinary bladder with optical coherence tomography: optical characterization of morphological changes. *Optics Express.* **10**, 1431-1443 (2002).
8. Barwari, K., *et al.* Differentiation between normal renal tissue and renal tumours using functional optical coherence tomography: a phase I in vivo human study. *BJU. Int.* **110**, E415-E420 (2012).
9. Barwari, K., *et al.* Advanced diagnostics in renal mass using optical coherence tomography: a preliminary report. *J. Endourol.* **25**, 311-315 (2011).
10. Cauberg, E. C., *et al.* Quantitative measurement of attenuation coefficients of bladder biopsies using optical coherence tomography for grading urothelial carcinoma of the bladder. *J. Biomed. Opt.* **15**, 066013 (2010).
11. Bus, M. T., *et al.* Volumetric in vivo visualization of upper urinary tract tumors using optical coherence tomography: a pilot study. *J. Urol.* **190**, 2236-2242 (2013).
12. Wessels, R., *et al.* Optical coherence tomography in vulvar intraepithelial neoplasia. *Journal of Biomedical Optics.* **17**, (2012).

13. Yun, S. H., Tearney, G. J., de Boer, J. F., Iftimia, N., Bouma, B. E. High-speed optical frequency-domain imaging. *Optics Express.* **11**, 2953-2963 (2003).
14. Kodach, V. M., Kalkman, J., Faber, D. J., van Leeuwen, T. G. Quantitative comparison of the OCT imaging depth at 1300 nm and 1600 nm. *Biomed. Opt. Express.* **1**, 176-185 (2010).
15. Kinkelder, R., de Bruin, D. M., Verbraak, F. D., van Leeuwen, T. G., Faber, D. J. Comparison of retinal nerve fiber layer thickness measurements by spectral-domain optical coherence tomography systems using a phantom eye model. *J. Biophotonics.* **6**, 314-320 (2013).
16. Baxter, G. M., Sihdu, P. S. *Ultrasound of the Urogenital System.* Thieme Medical Publishers Inc New York, United States (2006).

